IRS: the Spectrograph on SIRTF; Its Fabrication and Testing

J.R. Houck[a], T.L. Roellig[b], J. Van Cleve[a], B. Brandl[a], and K. Uchida[a]

[a] Cornell University, Ithaca, NY 14853
[b] NASA Ames Research Center, Moffitt Field, CA 94035

ABSTRACT

The Infrared Spectrograph, IRS, for SIRTF is a set of four compact low and medium resolution infrared spectrographs designed to work in the wavelength range from 5.3 to 40 μm at resolutions, $\lambda/\Delta\lambda$, from 65 to 600. The design involves all reflecting optics with no moving parts. The basic design philosophy, the fabrication process, the test program, and the real-time pointing capabilities are discussed.

Keywords: SIRTF, NASA, infrared, spectrograph, gratings

1. INTRODUCTION

The primary objective in the design of the IRS was to take maximal advantage of the very low background conditions provided by the space environment. The mid-infrared background in the SIRTF orbit is approximately 10^6 times smaller than the background at a modern ground-based facility. If the benefit of this reduced background is fully achieved, the enhancement in sensitivity is ~10^3, while the speed enhancement is ~10^6. The low resolution modules described below very nearly achieve the full benefit of the space environment, while the high resolution modules are detector dark-current limited.

The infrared spectrograph for SIRTF was heavily cost constrained. To reduce the number of initial design studies, a set of axioms was developed. These axioms were:

1. SIRTF is a cost driven mission.
2. Boeing Si:As and Si:Sb BIB arrays will be used.
3. The IRS will have aluminum structure and optics.
4. Only simple optics will be used.
    - Only surfaces of revolution (may be off axis)
    - Flat gratings
5. There will be no moving parts and no adjustments.
6. The IRS will be redundant only for credible single point failures.
7. The design will strive for an observing efficiency of >80%.
8. The IRS will be capable of internal health assessment.

The resulting design consists of four separate modules whose basic characteristics are summarized in Table 1. The finished, tested, and qualified modules are shown mounted on their flight baseplate in Figure 1. Sample images from two of the modules are shown in Figure 2.

The low resolution modules are long slit spectrographs with two slits each. Light passing through one slit is dispersed in first order while light passing through the other slit is dispersed in first and second order. Because the latter slit includes a small portion of the first order light, there is significant overlap between spectra taken through the two slits. This helps establish the relative amplitudes of the first and second order spectra. The high resolution modules have short slits which are roughly twice as long as their widths. A first order grating is used as the predisperser for the echelle which operates in 11^{th} through 20^{th} orders. The Short-Low module also has two imaging apertures to aid in source acquisition and telescope pointing. The interference filters used to block overlapping orders and to define the imaging band passes were manufactured by Optical Coating Laboratories, OCLI. The physical locations and orientations of the slits and apertures in the SIRTF focal plane can be found in the SIRTF Observer's Manual[1].

Table 1. Module Characteristics

Module	Wavelength Range (mm)	Pixel Size (arcsec)	Slit Width x Length (arcsec)	Spectral Resolution (l/Dl)
Short-Low	5.3 – 8.5 7.5 – 14.2	1.8 1.8	3.6 x 54.6 3.6 x 54.6	~65 to 115 ~65 to 115
Blue Peak-Up	13.3 – 18.7	1.8	60 x 72	NA
Red Peak-Up	18.5 – 21.8	1.8	60 x 72	NA
Long -Low	14.2 – 21.8 20.6 – 40.0	4.8 4.8	9.7 x 151.3 9.7 x 151.3	~65 to 115 ~65 to 115
Short – High	10.0 – 19.5	2.4	5.3 x 11.8	~600
Long – High	19.3 – 37.0	4.8	11.1 x 22.4	~600

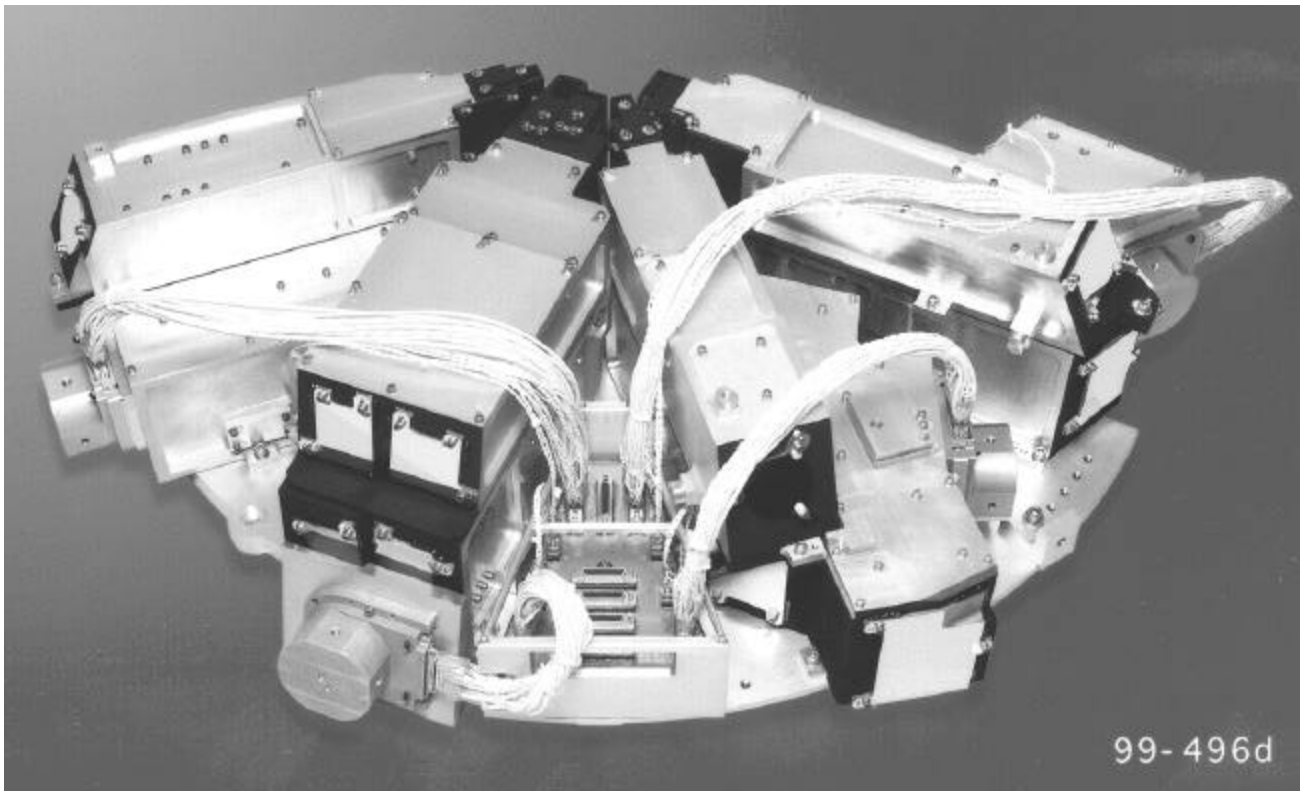

Figure 1. The four IRS modules mounted on their flight baseplate.

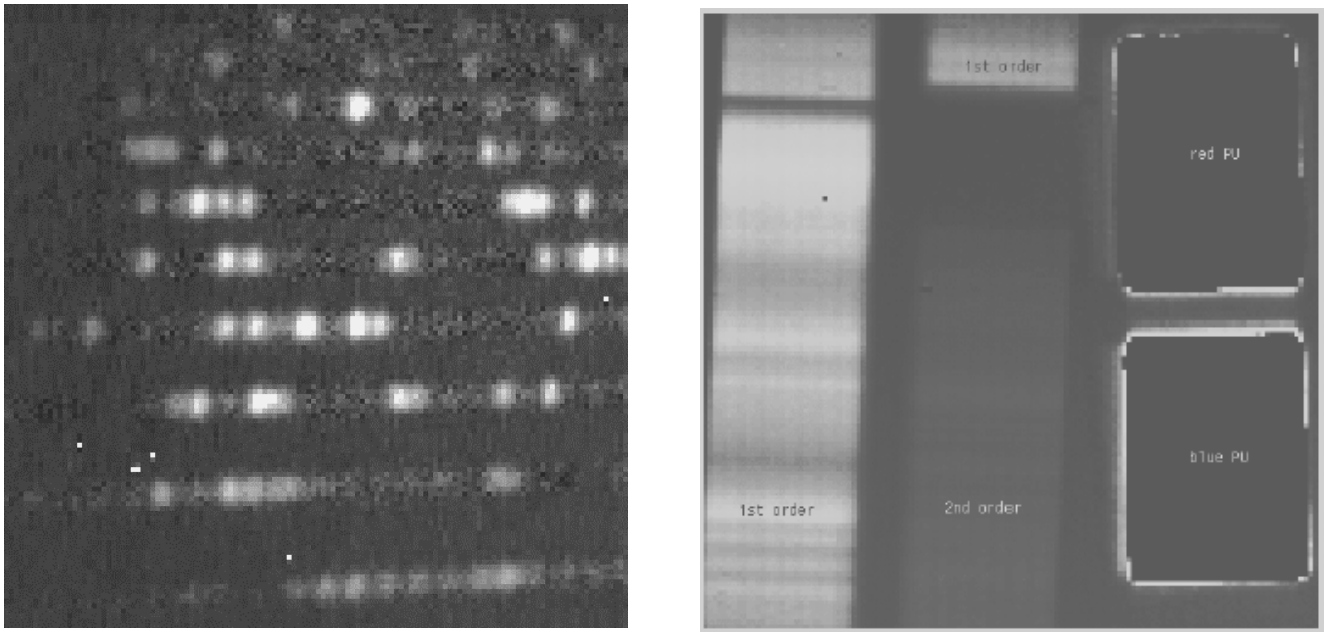

Figure 2. A sample spectrum from the Long-High module showing H_2O bands from a 300 mm pathlength in test-lab air. Note: many of the spectral lines are blends and/or pressure broadened. (left image). A sample image from the Short Low module showing first order on the left, second order and part of the first order in the middle and the peak-up apertures to the right. (right image) The peak-up apertures appear black because the displayed image is the difference of two images both of which are saturated in the peak-up aperatures. All spectra have longer wavelengths toward the bottom.

2. DETECTORS

The detectors were developed and manufactured by Boeing North America as part of an ongoing collaboration with Cornell University. Their general characteristics are summarized in Table 2.

Table 2. Detector Characteristics

Parameter	Si:As	Si:Sb	Units
Format	128 x128	128 x128	Pixels
Pixel Size	75 x75	75 x75	μm
Read noise	30	30	e^- / read
Dark Current	10	30	e^- / sec
DQE	50	40	%

A more complete discussion of the performance and clocking modes of the detectors can be found in the SIRTF Observers Manual[1], and Van Cleve et al[2].

3. FABRICATION

The individual modules are about the size of a shoe box. The housings were manufactured in two parts: an upper and lower housing. The housings were hogged out of aluminum blocks all cut from the same plate. They were first rough machined, and then heat treated to remove the stresses produced by the rolling and machining processes. The heat treated parts were then finish machined. Each module has between 8 and 12 baffle plates mounted more or less perpendicular to the ray bundles. Each baffle has 1 to 4 holes to pass the bundles at different locations along the optical path. The interiors of the housings and their baffles were painted black. The upper and lower housings are held together in a semi-kinematic way with screws and pins. A labyrinth joint between the housing sections allows trapped air to escape during pump down while preventing photons from entering the housings. The mirrors and gratings are mounted from the outside permitting easy replacement of an optic if need be. Three diamond turned tabs on the optics are held to matching lapped bosses on the housing exteriors with screws and pins. The backs of the optics were also diamond turned, they were checked interferometrically before and after an optic's installation to determine if the optics were distorted by the installation process. A similar three-pad scheme was used to mount the filter and slit holders to the housings. There are no provisions for adjusting the optics or apertures. A spacer plate between the housing and the focalplane array is custom machined to achieve proper detector focus and centering.

4. OPTICAL TESTING

The IRS was extensively tested for over a year in a series of fourteen separate cool downs in the IRS test facility at Ball Aerospace and Technologies Corp. In each of the approximately one week long cool downs one or more of the IRS modules was tested. Over this period there were hundreds of hours of testing during which, many thousands of images were recorded. The general testing procedures are described below. The requirements and actual performance figures are presented in the SIRTF Observer's Manual[1]

Although the main focus of this report is on the optical testing of the cryogenic parts of the IRS, the IRS/MIPS common electronics, CE, were used, and *de facto*, tested by the activities outlined below. Beginning in December 1999 all tests were run using TTACS and the Lockheed spacecraft simulator to operate the IRS. The actual flight electronics (including cables that simulate the flight cables) and the flight software were used during the last several cool downs. Although one can imagine improvements, our extensive experience has shown the IRS is convenient to command. We also find the data are free of annoying artifacts and easy to interpret.

The ideal test environment would be a fully cooled (~4K) test chamber that could accommodate the IRS cryogenic assemblies, and a series of test sources which delivered a properly configured beam to the module entrance apertures with a wide variety of selectable spectral and photometric characteristics. However, the cost of such a facility in terms of complexity, certification, schedule, and budget impact was prohibitive. In fact, just designing, building, and certifying such a cryogenic facility would be a task nearly as difficult as building the IRS itself. In keeping with the IRS axioms, a modular test approach was adopted in which many different optical configurations could be employed to generate a large quantity of data to certify the IRS modules. The turn-around time for any one cool-down was kept to a minimum. The quickest turn-around in the actual testing program was just six days.

The testing of the IRS was performed in the large clean room in the Fisher Test Building at Ball. The basic setup consisted of a Dewar capable of holding the entire IRS cold assembly of four modules, and the cold interface board mounted on the IRS flight baseplate. In addition, there were a number of ancillary infrared sources external to the Dewar which could be used to feed light into the IRS.

Janis Dewar:
The workhorse of the IRS test facility was the Janis Dewar. A schematic view of the filter stack inside of the Dewar is shown in Figure 3. The modules were mounted on the IRS baseplate which was in turn mounted on a cold fin inside the Dewar. The IRS was surrounded by a LHe cooled shield which was painted black on the inside. The IRS detectors routinely reached temperatures of ~5.5K.

Optical access to the modules was through a KRS-5 vacuum window, a set of LN_2 and LHe cooled thin film neutral density filters on silicon substrates, and a light-tight manually-operated LHe cooled door. Care was taken to minimize reflections

between the ND filters by tipping them and providing adaquate black surface area to absorb radiation reflected by the filters before it could get back into the optical path. Nonetheless, off-axis LN_2 radiation can be reflected *into* the optical path by the inner side of the LN_2 ND filter. This is a significant signal. However, the images of external sources are generally differences with the source "on" and "off." This subtraction removes the "false" cold radiation signal. Of course, the ND filters will be absent in the flight configuration!

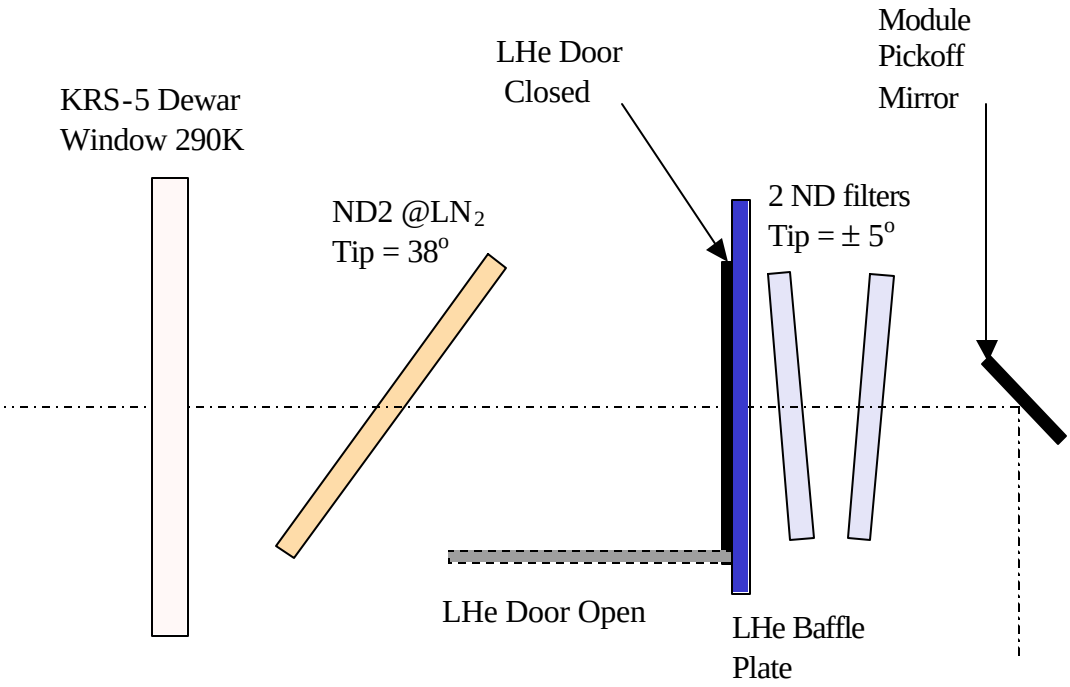

Figure 3. Schematic view of the window and filter stack in the Janis test Dewar. While the LN_2 was common to all modules, the Lhe filters were optimized for the individual modules.

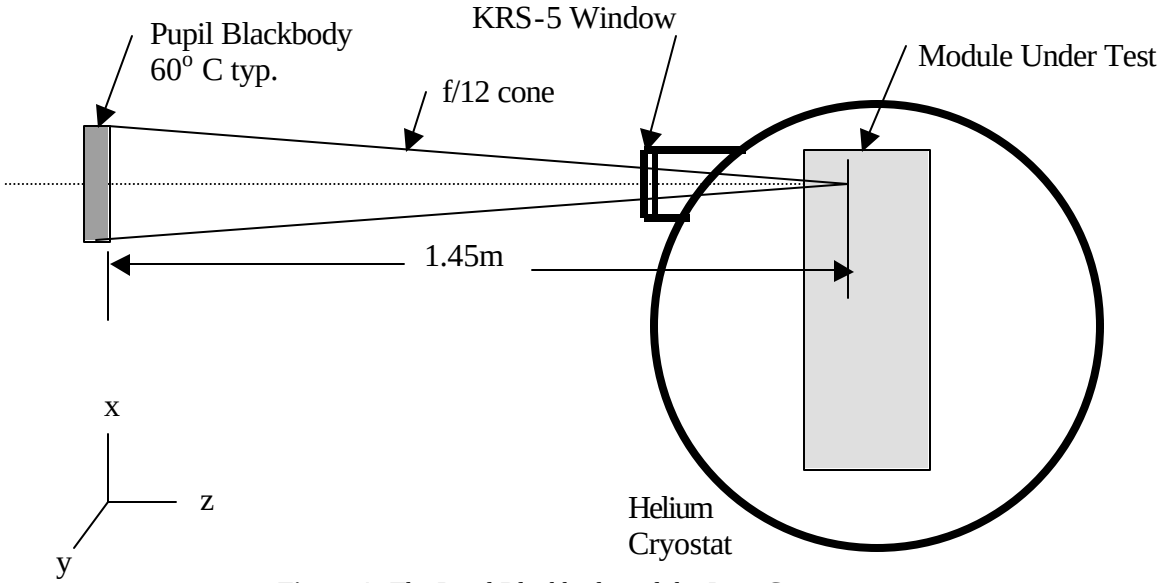

Figure 4. The Pupil Blackbody and the Janis Cryostat.

When the LHe door is closed the background in the modules is too small to be measured accurately. In this condition the read noise and an upper limit to the dark current performance were measured.

Pupil Blackbody:
A blackbody source with the diameter and relative location of the SIRTF Cryogenic Telescope Assembly, CTA, exit pupil produced a beam mimicking the radiation coming from an extended source as viewed by the CTA, see Figure 4. This custom-made pupil blackbody, PBB, could be moved toward and away from its nominal position (±Z) as well as in the plane of the CTA exit pupil (±X, Y) to map the shape of the modules' f-beams. This system was used to verify that the modules were all pointed in the same direction and toward the position of the exit pupil. Tests were performed to measure the emissivity of the PBB.

Point source projector:
An all reflecting optical system, using a spherical mirror, projected a point source image into the entrance apertures of the modules. Data from these tests were used to verify the focus of the modules. The point source projector was also used to make an end-to-end test of the peak-up system. A spot was projected into one of the peak-up windows, and the software was commanded to perform a peak-up operation. The source location returned by the peak-up software in the CE was then compared to the location of the point source image as determined by more conventional image processing. The accuracies of these comparisons were consistent with the thousands of computer simulations of the peak-up process which were performed on simulated peak-up images.

Monochromator:
A commercial grating monochromator was available to feed light into the point source projector and from there to the module apertures. The monochromator was run at high order whenever possible to project multiple wavelengths into the apertures at once. These tests determined the dispersion curves for the spectrographs. A variety of slits and gratings were available for the monochromator to cover the IRS' wavelengths and resolutions. In addition, a set of $\lambda/\Delta\lambda \sim 10$ interference filters from OCLI was used to check the dispersion properties of the modules. Because the filters transmitted far more light than the monochromator, they were used to search for ghost images.

5. IRS PERFORMANCE TESTING

The methods used to verify the performance of the IRS are described below.

Detector Properties:
The three fundamental detector properties, read noise, dark current and responsivity were measured with the modules in the flight condition in the Janis Dewar using the CE, S/C simulator, and TTACS. Dark current and read noise were measured by closing the LHe temperature door and making exposures at all available exposure times up to and including 500 seconds. The combined noise was below the requirement. The responsivity was measured in an end-to-end way by exposing the modules to the PBB at a temperature of 60°C and then blocking the PBB and making a second exposure to the room radiation at a temperature of 23°C. Extracting the responsivity from these measurements required knowledge of the transmission of the ND filters in the Dewar. These curves were measured by their manufacturers, Janos and DSI. They were independently measured at the University of Rochester by Dan Watson. The total ND stack varied from ND = 4 for the S-H to ND = 6 for the S-L peak-up. The end-to-end transmission agreed with model calculations.

Each module contains a flood illuminator to monitor the responsitivity stability. Data taken over several months show the response to the stimulator remained constant within $\leq 1\%$.

Spectral resolution:
The module spectral resolution was measured by the monochromator, and by measuring the line widths from gas cell absorption spectra. H_2O, CO_2 and NH_3 were used as absorbers. The H_2O spectrum was obtained by subtracting pairs of exposures taken with the PBB-to-Dewar distances which differ by 300mm. The slight difference in the atmospheric absorption over this 300mm path was sufficient to achieve good signal to noise as shown in Figure 2. The CO_2 and NH_3 spectra were obtained by placing a block of dry ice or a dish of household ammonia near the Janis Dewar window. A small cardboard shield prevented room room air currents from dispersing the gasses too quickly. The resolutions listed in Table 1 were achieved.

Wavelength Coverage:
The data from the spectral resolution tests were also used to derive dispersion curves for the low resolution modules. Similar data for the high resolution modules were compared to the Code V raytraces for the modules. In all cases the observed and

predicted wavelength coverages agreed. The only deviation from the formal requirements was that the short wavelength limit of the S-L module was 5.3 microns rather that the specified 5 microns. This deviation was driven by the need to avoid out-of-order leakage in the S-L.

Sensitivity:
Verification of the photometric sensitivity was accomplished by measuring the differential response to the PBB and the ambient BB radiation from the room.

Focus:
The focus verification entails two different aspects of the IRS: the IRS focus position relative to the CTA focus, and the focus within the individual modules. The first is determined warm. Because all the modules have entrance slits (or apertures in the case of the peak-up) preceding the blocking filters in their optical paths, the slits and apertures can be directly viewed from outside using an optical microscope. Because the system is all aluminum, the CTE mismatch is very small, and thermal induced strains are much smaller than the CTA depth of field.

The focus within the modules was verified with the modules cold. This was accomplished by observing the sharpness of narrow spectral features in the gas absorption spectra, by observing the sharpness of the edges of the peak-up windows and the ends of the slits in detector images. In the first case the Code V PSF could be used to compare the sharpness of the spectral feature for a point source illumination. In the second case, the Laplace transform of the Code V PSF was compared to the observed edge drop offs.

f-beam mapping:
The PBB was used to map the shape and size of the f-beam. With the PBB at the nominal position of the CTA exit pupil relative to the entrance apertures, it was scanned in X and Y (see Figure 4) to find the maximum response for each module. Once the maximum was found, scans were made to map the shape of the f-beam. These scans were compared to model plots of the anticipated f-beam at the CTA exit pupil. Consistent agreement was achieved.

Scattered/Stray Light:
Because the IRS spectrographs do not contain Lyot stops, they have significant sensitivity to radiation outside their f/12 acceptance cones. The out-of-the-f-cone response was measured with the PBB by scanning it in X, Y, and Z. The system, IRS plus CTA, off-axis response was calculated by convolving the measures out-of-the-f-cone response with the predicted stray light distribution within the CTA.

6. THE PEAK-UP MODE

The Short-Low module is equipped with two imaging paths in addition to its first and second order spectral paths. An accurate position of a source can be determined by first imaging it through one or the other of the peak-up cameras. The images are then processed onboard the spacecraft in real-time using the peak-up algorithm. The algorithm locates the brightest point like source in the field and determines its centroid. This centroid is then sent to the spacecraft's pointing control system, and it is used in offsetting from the peak-up FOV to the appropriate slit.

The peak-up algorithm works by thresholding the peak-up images, effectively flooding the image to submerge the low level point and extended sources, and thereby isolating the brighter point-like and slightly extended sources form the general background. This process produces an accurate centroid at the expense of relatively poor photometric accuracy.

The process begins with by taking three images using double correlated sampling: DCS1, DCS2, and DCS3. The algorithm then –

1) produces there difference images, DSC1– DCS2, DCS2 – DCS3, and DCS3 – DCS1. These three difference images contain only noise and cosmic ray (CR) effects since any photocurrent signal is "subtracted out." Note: shot noise form photocurrent will be present. The out-liers at the top and bottom of the pixel value distribution are presumed to result from cosmic rays.
2) replaces the known bad pixel values, and calculates the variance, σ^2, of the pixel values while ignoring the out-lyers identified in step 1,
3) removes mean and any planar background from the original images,

4) identifies as CR hits all pixel locations which have difference image values outside of ±3.5σ. The pixel values for these locations are set to zero in the zero mean images produced in step 3.
5) convolves each zero-mean-frame with the appropriate PSF (red or blue), and then sums the three images,
6) identifies clusters of pixels in the summed image that exceed the threshold signal value. Clusters with too few pixels to be legitimate infrared point sources are presumed to be residual CR effects, or other noise glitches, which have escaped the earlier processing. These pixels are also set to zero.
7) finds the centroid of the remaining cluster with the greatest peak flux. Pixels which do not exceed the threshold are ignored.

The resulting centroid is used by the spacecraft to calculate the offset to the desired slit. In most cases, a point source between 1 and 2 mJy is sufficient to achieve an accurate peak-up position. However, a brighter source is required in very crowded regions, or in regions where the 100μm cirrus is in exc ess of ~100 MJy/sr.

7. SUMMARY

Although the IRS was heavily cost constrained, the final instrument meets the primary goal of maximally exploiting the low background conditions in the SIRTF orbit. The IRS hardware meets the design predictions, and it will provide spectra of unprecedented sensitivity when successfully placed in orbit around the Sun.

8. ACKNOWLWDGEMENTS

The IRS benefited greatly from highly skilled and dedicated teams at Ball Aerospace and Technologies Corporation, Boeing Research and Technology Center, and Optical Coating Laboratories Incorporated. Their hard work enabled the IRS to achieve its technical, financial and schedule objectives. This paper is dedicated to the memory of Dave Seib who was instrumental in the development of the blocked impurity band silicon detectors used in the IRS. Dave was wonderful source of good ideas, constant inspiration, and skilled leadership for more than a decade. This project was supported by NASA through JPL Contract 960803.

9. REFERENCES

1. SIRTF Observers Manual , SIRTF Science Center, California Institute of Technology, Pasadena, CA available at http://sirtf.caltech.edu/SciUser/Documents/SOM.html

2. Van Cleve, J.E., Herter, T.L., Butturini, G., Gull, G.E., Houck, J.R., Perger, B., and Schoenwald, J., 1995 Proc. SPIE Vol. 2553, p.502-513